Accuracy of dose calculation based on artefact corrected Cone Beam CT images of lung cancer patients

Slot Thing, Rune; Bernchou, Uffe; Hansen, Olfred; Brink, Carsten

Published in:
Physics and Imaging in Radiation Oncology

DOI:
10.1016/j.phro.2016.11.001

Publication date:
2017

Document version
Publisher's PDF, also known as Version of record

Physics and Imaging in Radiation Oncology 1 (2017) 6–11

Contents lists available at ScienceDirect

Physics and Imaging in Radiation Oncology

journal homepage: www.elsevier.com/locate/phro

Original Research Article

Accuracy of dose calculation based on artefact corrected Cone Beam CT images of lung cancer patients

Rune Slot Thing [a,b,*], Uffe Bernchou [a,b], Olfred Hansen [a,c], Carsten Brink [a,b]

[a] Department of Clinical Research, University of Southern Denmark, DK-5000 Odense, Denmark
[b] Laboratory of Radiation Physics, Odense University Hospital, DK-5000 Odense, Denmark
[c] Department of Oncology, Odense University Hospital, DK-5000 Odense, Denmark

ARTICLE INFO

Article history:
Received 9 August 2016
Received in revised form 11 November 2016
Accepted 30 November 2016

Keywords:
Image guided radiotherapy
Adaptive radiotherapy
Dose of the day
Cone Beam CT

ABSTRACT

Background and purpose: Accurate Cone Beam CT (CBCT) based dose calculations are hindered by limited CBCT image quality. Using retrospective artefact corrections, this paper investigated the accuracy of dose calculations performed directly on CBCT images of lung cancer patients.

Materials and methods: Dose calculations were made directly on clinical and artefact corrected CBCT images of 21 lung cancer patients with a re-simulation CT (rCT) image acquired during radiotherapy. The original treatment plan was copied to the rCT and CBCT images and dose was recalculated. Dose comparisons were made using gamma analysis and dose statistics. Gamma comparisons were made using 2%/2 mm and 1%/1 mm criteria, and pass rates of the clinical and improved CBCT images were calculated using the rCT based dose as reference.

Results: Dose distributions calculated on the artefact corrected CBCT images had a median 2%/2 mm gamma pass rate of 99.4% when compared to the reference rCT. Doses calculated on the clinical CBCT images had a median 2%/2 mm gamma pass rate of 93.1%. Wilcoxon signed rank test showed the pass rates in the entire CBCT field of view different at $p < 0.001$. Clinical CBCT image based dose calculations overestimated the dose, while the improved CBCT doses were in closer agreement with the rCT doses.

Conclusions: Comprehensive artefact correction of CBCT images allowed highly accurate dose calculations to be performed directly on CBCT images of lung cancer patients, following the standard CT-based workflow in a treatment planning system.

1. Introduction

Over the last decade, research in Cone Beam CT (CBCT) based adaptive radiotherapy (ART) has seen a growing interest. Different uses of the three dimensional anatomical information obtained through CBCT based image guided radiotherapy (IGRT) have been investigated, such as CBCT based dose calculations [1–5] and tumour and normal tissue response during fractionated radiotherapy [6–9].

The one common factor which inhibits the clinical realisation of CBCT based ART is the image quality of CBCT images. A multitude of artefacts and lack of proper Hounsfield Unit (HU) calibration means that the standard tools developed in radiotherapy for use with fan beam CT images cannot be transferred directly to CBCT images. Several papers have been published demonstrating how artefact corrections or alternative HU to electron density tables can compensate for the limited CBCT image quality and allow dose calculations to be performed either directly on the CBCT images [2–4,10] or on CT images adapted to correspond to the anatomy as seen on the daily CBCT scan [1].

This study investigated the accuracy of dose calculations performed directly on thoracic CBCT images subjected to comprehensive artefact corrections. Following the artefact corrections, dose calculations were made following the standard CT-based workflow in a treatment planning system. CBCT based doses were compared to CT based dose calculations using gamma analysis, as well as dose statistics.

2. Methods

A total of 21 lung cancer patients treated for non-small cell lung cancer (NSCLC) with 66Gy in 33 fractions at Odense University

* Corresponding author at: Department of Medical Physics, Vejle Hospital, DK-7100 Vejle, Denmark.
E-mail address: rune.slot.thing@rsyd.dk (R.S. Thing).

http://dx.doi.org/10.1016/j.phro.2016.11.001

Hospital between January 2013 and December 2015 were included in the present study. Based on clinical indications, all patients had a re-simulation CT (rCT) acquired during treatment.

For each patient, a CBCT scan was acquired for IGRT on the day of rCT imaging, using our standard clinical protocol for fast 4D CBCT acquisition on Elekta Synergy or Versa HD accelerators equipped with XVI R4.5 or R5.0 (Elekta AB, Stockholm, Sweden). Approximately 750 projection images spanning an arc of 220 degrees were acquired over 2.2 min scan time, using the S20 collimator and F0 filter cassettes. From version 5.0, the XVI software has a feature called HU calibration, which uses an image of a homogeneous phantom to correct for some generic artefacts. While this approach may be successful in recovering CBCT HUs when a patient is well represented by the homogeneous phantom used for calibration, it does not ensure a HU-calibrated CBCT scan for all patients. This feature was not used for reconstruction of any CBCT scans in the present study, as the feature was not available at the start of the project.

2.1. Image processing

To allow dose calculations on the CBCT images, each clinical CBCT image was reconstructed to an average 3D CBCT using the XVI software. This reconstruction was referred to as the *clinical CBCT*. Additionally, an artefact corrected CBCT image was reconstructed using our previously developed framework [11]. This corrected reconstruction was based on extraction of the clinical CBCT projection images, which were then corrected for image lag, detector scatter, patient body scatter and beam hardening, as well as re-scaling of the pixel values prior to average 3D reconstruction. Corrections for image lag and detector scatter were performed using empirical models developed for the flat panel detectors in our clinic, while corrections for patient body scatter and beam hardening were based on patient specific Monte Carlo simulations of primary and scattered photons. The image corrections required only the original CBCT projection images as well as the initial planning CT to be performed. CBCT reconstructions of these *improved CBCT* images were made using the filtered backprojection algorithm implemented in the Reconstruction Toolkit [12].

To minimise the small residual anatomical differences between the CBCT and rCT images acquired on the same day (respiratory motion, baseline shifts, different positioning on the couch etc.), the CBCT images were deformably registered against the rCT image using elastix [13]. Deformable image registrations were made using the settings of a parameter file obtained from the elastix wiki website [14], and validated by Klein et al. to have a median residual mismatch of about 1 mm in the chest region when used for CT to CT based deformable registration [13].

With the CBCT images acquired in the small field of view on the XVI system, the CBCT images suffered from truncation of the anatomy. To allow dose calculations to be performed, the missing anatomy in the CBCT images was padded from the rCT, to which the CBCT images had already been deformably registered. This last step was referred to as embedding in the rCT image, and the full process is shown in Fig. 1. The resulting CBCT images were referred to as cCBCT (clinical CBCT) and iCBCT (improved CBCT).

2.2. Dose calculations

The original treatment plan (single or dual arc VMAT, planned on the mid-ventilation phase of a 4D CT) was copied to the rCT, iCBCT and cCBCT image sets, and dose was calculated on all three image sets using the collapsed cone algorithm in Pinnacle with a $3 \times 3 \times 3$ mm^3 dose grid. No plan optimisation was performed in this recalculation study; only the isocenter, beams, and monitor units were transferred from the original dose plan. The rCT and CBCT images were handled in exactly the same way during dose calculation, using our standard CT to electron density conversion curve for dose calculation on the rCT and CBCT images.

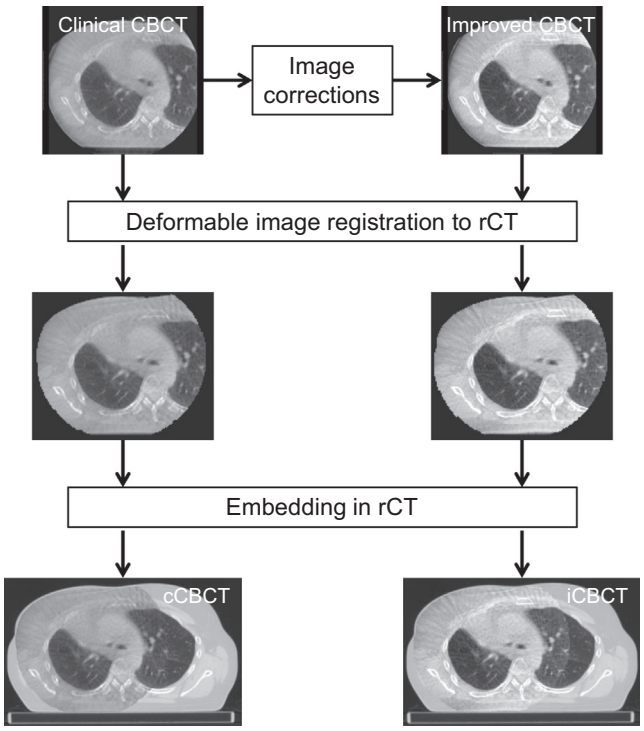

Fig. 1. Two CBCT images were prepared for dose calculation for each patient. The clinical CBCT projection images were subject to extensive image corrections before being reconstructed to produce the improved CBCT. The clinical and improved CBCT images were then deformably registered to the re-simulation CT (rCT) acquired on the same day as the CBCT image projections. To compensate for the truncated field of view of the CBCT images, the missing anatomy in the deformed CBCT images was added from the rCT image to produce the cCBCT (clinical) and iCBCT (improved) images ready for dose calculation.

2.3. Evaluation of calculated doses

The calculated dose distributions were compared using 3D gamma analysis [15–17] at the 2%/2 mm and 1%/1 mm level. The rCT based dose was used as reference, while the cCBCT and iCBCT doses were used as evaluated doses. Dose matrices were resampled to a finer grid size using trilinear interpolation to a $(0.45\ \text{mm})^3$ grid to allow the strict distance to agreement criteria to be evaluated. A low dose threshold of 10% of the prescription dose was applied for the gamma calculations, and the dose difference criterion was calculated using the prescribed dose of 66 Gy. Gamma values were only calculated within the volume where HU values originated from the CBCT images, and gamma pass rates (percentage of gamma values below 1) were used to assess the dose calculation accuracy of the CBCT images.

To evaluate potential anatomical dependencies of the CBCT based dose calculation accuracy, gamma pass rates were further calculated within the delineated PTV, lungs, heart, spinal cord, and oesophagus. Organs were delineated on the rCT, and due to the deformable image registration of the cCBCT and iCBCT images, the structures were directly transferable to the CBCT image sets.

Dose volume histograms (DVHs) were produced to relate the gamma pass rates to a clinically relevant measure. To simplify the comparison of dose volume metrics, dose statistics of target coverage and organs at risk dose volumes were calculated and

compared between the rCT and the CBCT based doses. Dose statistics were chosen according to the constraints used for treatment planning of NSCLC in our clinic.

2.4. Statistical analysis

To assess the difference between gamma pass rates for doses calculated on the cCBCT and iCBCT images, statistical analysis was performed using the Wilcoxon signed rank test. Statistical analyses were made in Matlab R2014a (The Mathworks Inc, Natick, MA, USA).

3. Results

An illustrative example of the calculated dose distributions, dose differences and gamma values is shown in Fig. 2. The patient shown in Fig. 2 was selected as one of the patients with the largest difference between the CT and CBCT based doses. The cCBCT based dose was found too high compared to the reference dose calculated on the rCT image, which was the general trend observed for the cCBCT based dose calculations in this study. The iCBCT based dose distribution was much closer to the reference dose, which was also reflected in the gamma values being lower for the iCBCT based dose compared to the cCBCT based dose.

The median gamma pass rate at the 2%/2 mm level in the entire CBCT volume was 93.1% for the cCBCT based doses and 99.4% for the iCBCT based doses. The mean of the actual mean gamma value for the 21 patients at 2%/2 mm was 0.39 ± 0.04 (mean ± standard error) for the cCBCT based doses, and 0.21 ± 0.01 for the iCBCT based doses. At 1%/1 mm, the median pass rates were 79.9% and 94.8% for the cCBCT and iCBCT based doses. The mean of the mean gamma values for all patients was 0.79 ± 0.07 and 0.39 ± 0.03 for the cCBCT and iCBCT based doses. Wilcoxon signed rank statistics showed the median gamma pass rates different at $p < 0.001$ at both the 2%/2 mm and 1%/1 mm level. Fig. 3 shows the gamma pass rates for the entire CBCT volume, as well as for individual organs. It is evident that the image quality improvements applied to the iCBCT images caused an increase in median gamma pass rate for all organs at both the 2%/2 mm and 1%/1 mm level, as well as a reduction in the interquartile range.

Fig. 4 shows a DVH calculated for the same patient as shown in Fig. 2. As with the dose visualisation, the DVH plot shows that the cCBCT image resulted in too high doses being calculated. The iCBCT

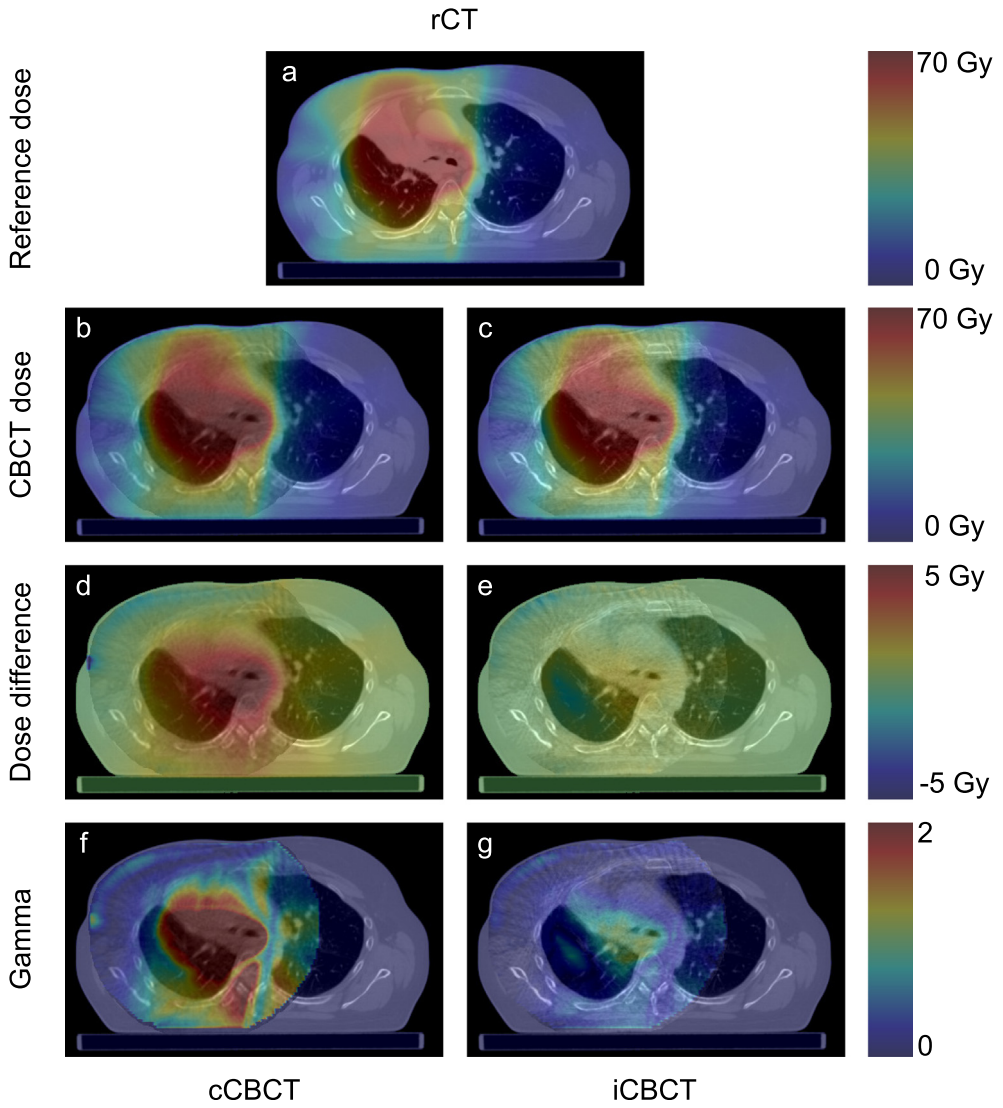

Fig. 2. Illustrative example dose distribution as calculated on the rCT (a), cCBCT (b), and iCBCT (c) image sets. Dose difference in the example slice is show in (d) (cCBCT-rCT) and (e) (iCBCT-rCT), while (f)-(g) show the 2%/2 mm gamma values for the cCBCT and iCBCT dose distributions calculated using the rCT dose as reference dose.

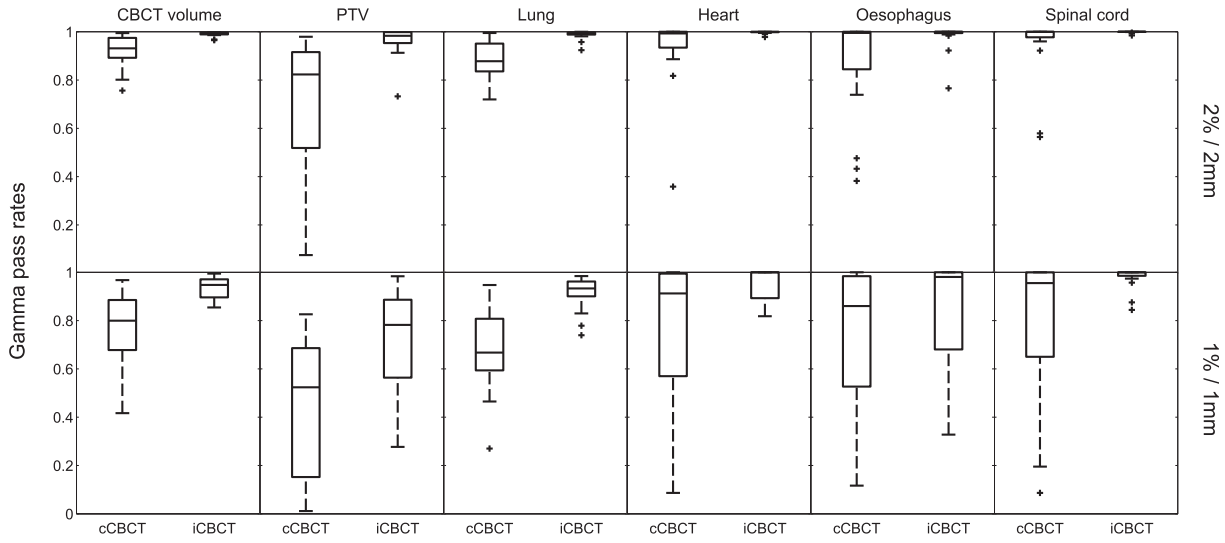

Fig. 3. Box plots of 2%/2 mm (top) and 1%/1 mm (bottom) gamma pass rates for the entire CBCT field of view as well as for individual structures as delineated on the rCT images. Wilcoxon signed rank tests indicated statistically significant different median values at $p \leqslant 0.01$ for all plots, except oesophagus where the 1%/1 mm gamma pass rates were different at $p = 0.03$. Whiskers indicate the most extreme value within 1.5 times the interquartile range from the 25th and 75th percentiles.

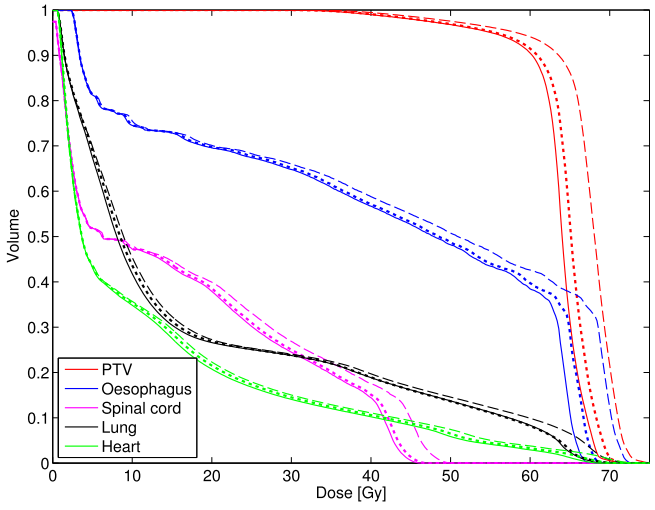

Fig. 4. Dose-volume histograms for an example patient. Solid line is dose calculated on the rCT image, long dashed line is dose calculated on the cCBCT image, and short dashed line is dose calculated on the iCBCT image.

based dose distribution provided DVH curves closer to the rCT based dose distribution, but still with slightly elevated dose levels at high doses. This illustrative case was selected as one of the patients with the largest CBCT to CT DVH differences found in the studied population. To couple the observed differences in gamma pass rates to a clinically relevant measure, differences in dose statistics as used in our clinic during treatment planning are reported in Fig. 5. Dose statistics were calculated on each rCT and CBCT based dose, before the rCT based dose statistics were subtracted from the CBCT based dose statistics. In general, both sets of CBCT based dose calculations provided dose statistics close to the rCT based doses, but it is evident that both accuracy and precision was improved when using the iCBCT images for dose calculation compared to using the cCBCT images.

4. Discussion

A median 2%/2 mm gamma pass rate of 99.4% for dose calculated directly on CBCT images of lung cancer patients compared to dose calculated on a CT image holds promise of an accurate way to determine the delivered rather than the planned dose to targets and organs at risk. For lung cancer patients with tumours that can move between fractions, it is of great interest to be able to do easy and accurate dose calculations to determine whether shifts in tumour position and/or patient anatomy in general has dosimetric effects on the prescribed treatment plan. While this can be done using repeat CT imaging, the reduced workload of being able to use CBCT images for dose calculation implies that systematic dose tracking for all patients is more readily achievable. Furthermore, the proposed methodology allows retrospective analysis of the dose delivered to patients who have already completed treatment since the iCBCT images were reconstructed from the existing clinical projection images. While no explicit study of the time stability of the used artefact corrections was carried out,

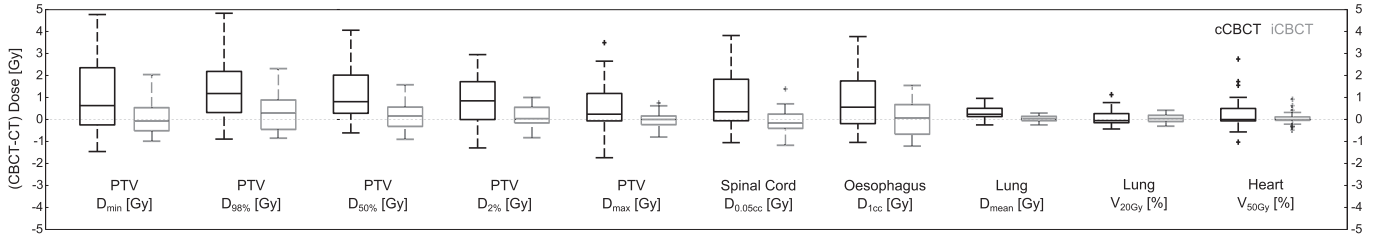

Fig. 5. Box plots of dose statistics differences for the cCBCT and iCBCT based dose calculations. Dose statistics were calculated on each of the CBCT and rCT based doses and subsequently subtracted. Comparisons were made within the part of the delineated structure that was within the CBCT field of view.

we note that the corrections have been used with the same calibration parameters on all linacs in our clinic. Artefact corrections have thus been performed successfully on XVI systems with detector panels three to eight years old at the time of image acquisition.

The present study showed that comprehensive artefact corrections in chest CBCT allows for accurate dose calculations to be performed directly on the CBCT images. Deformable registration between CT and CBCT images acquired on the same day was used to emphasize the accuracy of dose calculations based on the artefact corrected CBCT images. The residual misalignment following deformable registration using the same parameters as in the present study has been reported to be approximately 1 mm for the chest region [13] and 2–3 mm in the head and neck region [18] when registering CT scans against CT scans. The remaining inaccuracy in the alignment of the registered image sets motivated the use of gamma pass rates with distance-to-agreement criteria of 1 and 2 mm, to account for residual misalignment of the images. The choice of deforming the CBCT images to the rCT images was made to ensure that the image being deformed was the smaller volume of the two images being co-registered. If the rCT images were to be deformed, the part of the rCT image outside the CBCT FOV would be at risk of running wild during the deformable registration, as the cost function would only penalise voxels within the CBCT FOV if they were deformed too much. Individual deformable registrations of the cCBCT and iCBCT images were made to eliminate any registration bias towards either of the CBCT reconstructions, and in practice only very minor differences were observed when comparing the registrations of the cCBCT and iCBCT images from the same patient.

rCT and CBCT images were acquired on the same day to maximise the likeness of the images. It is however noted that the rCT images were acquired as 4D CT scans with the mid-ventilation phase used for dose calculation, while the CBCT images were reconstructed as average 3D scans. This implies that motion artefacts were present in the CBCT scans, but not in the rCT scans, potentially leading to an apparent enlargement and dilution of the tumour. Motion artefacts could, at least to some extent, explain why the gamma pass rates were lower for the PTV than for any other delineated structure, as such artefacts may be observed around the moving tumour.

While the present study was limited in the comparison of CT and CBCT images acquired on the same day, it demonstrated high accuracy of CBCT based dose calculations based on the iCBCT images. To move forward towards CBCT-only guided ART, a clinical study should be performed to investigate whether the iCBCT based dose calculations and potential plan reoptimisations result in similar clinical decisions as rCT based dose calculations. Further studies are also needed to assess how the adding of missing anatomy from the planning CT image rather than the rCT image affects the calculated dose–volume histograms and gamma comparisons between CBCT and CT based dose calculations. However, most often only small segments of the VMAT treatment pass through anatomy not contained in the CBCT FOV, and hence we expect only small changes to arise from using the planning CT for embedding. Extensions of the proposed methodology to other anatomical sites should be straight forward, since the chest region is recognised as the most difficult anatomical site for accuracte dose calculation [19,20].

Using artefact corrected CBCT images for dose calculation has the appeal that all existing clinical workflows need not change to accommodate the iCBCT images, which makes for an easy integration into any clinic regardless of treatment planning system etc. Furthermore, no CBCT- or patient specific HU to electron density conversion curve is required, as the standard CT conversion was used in the present study. Previous studies have suggested using deformable registration of the planning CT image to CBCT images to create a HU-accurate image of the daily anatomy for dose calculation [1,21], but it remains unclear how this methodology handles larger anatomical changes as well as changes in lung density observed during the course of treatment [6]. Using the artefact corrected CBCT images directly ensures the most accurate image of the daily anatomy. The present study reports higher gamma pass rates and smaller dose differences between the iCBCT based dose and the reference rCT based dose than what has been reported previously in CBCT recalculation studies of lung cancer patients [3,22–24].

This study demonstrated that the image quality of chest CBCT images can be recovered to allow highly accurate CBCT based dose calculations. Dose of the day calculations as well as dose accumulation studies are now within reach in a clinical environment. The main limiting factor in realising routine dose accumulation for all treated lung cancer patients is the delineation of target and organs at risk on the daily CBCT images. A combination of the present study and accurate auto-segmentation algorithms could be a promising way towards a low-cost high-accuracy method providing an accurate picture of what dose we deliver to every lung cancer patient treated with radiotherapy.

Acknowledgements

CB, RST, and UB acknowledge research support from Elekta Ltd. RST acknowledges PhD funding from Odense University Hospital and CIRRO – The Lundbeck Foundation Center for Interventional Research in Radiation Oncology and The Danish Council for Strategic Research. CB and OH acknowledge support from AgeCare (Academy of Geriatric Cancer Research), an international research collaboration based at Odense University Hospital, Denmark.

References

[1] Yang Y, Schreibmann E, Li T, Wang C, Xing L. Evaluation of on-board kV cone beam CT (CBCT)-based dose calculation. Phys Med Biol 2007;52:685–705.
[2] Rong Y, Smilowitz J, Tewatia D, Tomé WA, Paliwal B. Dose calculation on kV cone beam CT images: an investigation of the HU-density conversion stability and dose accuracy using the site-specific calibration. Med Dosim 2010;35:195–207.
[3] Fotina I, Hopfgartner J, Stock M, Steininger T, Lütgendorf-Caucig C, Georg D. Feasibility of CBCT-based dose calculation: comparative analysis of HU adjustment techniques. Radiother Oncol 2012;104:249–56.
[4] Elstrm UV, Olsen SRK, Muren LP, Petersen JBB, Grau C. The impact of CBCT reconstruction and calibration for radiotherapy planning in the head and neck region - a phantom study. Acta Oncol 2014;53:1114–24.
[5] Vestergaard A, Muren LP, Sndergaard J, Elstrm UV, Hyer M, Petersen JB. Adaptive plan selection vs. re-optimisation in radiotherapy for bladder cancer: a dose accumulation comparison. Radiother Oncol 2013;109:457–62.
[6] Bertelsen A, Schytte T, Bentzen SM, Hansen O, Nielsen M, Brink C. Radiation dose response of normal lung assessed by Cone Beam CT – a potential tool for biologically adaptive radiation therapy. Radiother Oncol 2011;100:351–5.
[7] Brink C, Bernchou U, Bertelsen A, Hansen O, Schytte T, Bentzen SM. Locoregional control of non-small cell lung cancer in relation to automated early assessment of tumor regression on cone beam computed tomography. Int J Radiat Oncol Biol Phys 2014;89:916–23.
[8] Bernchou U, Hansen O, Schytte T, Bertelsen A, Hope A, Moseley D, et al. Prediction of lung density changes after radiotherapy by cone beam computed tomography response markers and pre-treatment factors for non-small cell lung cancer patients. Radiother Oncol 2015;117:17–22.
[9] Jabbour SK, Kim S, Haider SA, Xu X, Wu A, Surakanti S, et al. Reduction in tumor volume by cone beam computed tomography predicts overall survival in non-small cell lung cancer treated with chemoradiation therapy. Int J Radiat Oncol Biol Phys 2015;92:627–33.
[10] Poludniowski GG, Evans PM, Webb S. Cone beam computed tomography number errors and consequences for radiotherapy planning: an investigation of correction methods. Int J Radiat Oncol Biol Phys 2012;84:e109–14.
[11] Thing RS, Bernchou U, Mainegra-Hing E, Hansen O, Brink C. Hounsfield unit recovery in clinical Cone Beam CT images of the thorax acquired for image guided radiation therapy. Phys Med Biol 2016;61:5781–802.
[12] Rit S, Oliva MV, Brousmiche S, Labarbe R, Sarrut D, Sharp GC. The Reconstruction Toolkit (RTK), an open-source cone-beam CT reconstruction toolkit based on the Insight Toolkit (ITK). J Phys Conf Ser 2014;489:012079.
[13] Klein S, Staring M, Murphy K, Viergever MA, Pluim JPW. elastix: a toolbox for intensity-based medical image registration. IEEE Trans Med Imag 2010;29:196–205.

[14] Klein S, Staring M, Murphy K, Viergever MA, Pluim JPW. Elastix parameter file par0003.bs-R6-ug.txt. Available at http://elastix.bigr.nl/wiki/images/0/04/Par0003.bs-R6-ug.txt. Accessed 2 November 2016
[15] Low DA, Harms WB, Mutic S, Purdy JA. A technique for the quantitative evaluation of dose distributions. Med Phys 1998;25:656–61.
[16] Low DA, Dempsey JF. Evaluation of the gamma dose distribution comparison method. Med Phys 2003;30:2455–64.
[17] Wendling M, Zijp LJ, McDermott LN, Smit EJ, Sonke JJ, Mijnheer BJ, et al. A fast algorithm for gamma evaluation in 3D. Med Phys 2007;34:1647–54.
[18] Zukauskaite R, Brink C, Hansen CR, Bertelsen A, Johansen J, Grau C, et al. Open source deformable image registration system for treatment planning and recurrence CT scans: validation in the head and neck region. Strahlenther Onkol 2016;192:545–51.
[19] Knöös T, Wieslander E, Cozzi L, Brink C, Fogliata A, Albers D, et al. Comparison of dose calculation algorithms for treatment planning in external photon beam therapy for clinical situations. Phys Med Biol 2006;51:5785–807.
[20] Fogliata A, Vanetti E, Albers D, Brink C, Clivio A, Knöös T, et al. On the dosimetric behaviour of photon dose calculation algorithms in the presence of simple geometric heterogeneities: comparison with Monte Carlo calculations. Phys Med Biol 2007;52:1363–85.
[21] Zhao W, Brunner S, Niu K, Schafer S, Royalty K, Chen GH. Patient-specific scatter correction for flat-panel detector-based cone-beam CT imaging. Phys Med Biol 2015;60:1339–65.
[22] Richter A, Hu Q, Steglich D, Baier K, Wilbert J, Guckenberger M, et al. Investigation of the usability of cone beam CT data sets for dose calculation. Radiat Oncol 2008;3:42.
[23] Amit G, Purdie TG. Automated planning of breast radiotherapy using cone beam CT imaging. Med Phys 2015;42:770–9.
[24] Dunlop A, McQuaid D, Nill S, Murray J, Poludniowski G, Hansen VN, et al. Comparison of CT number calibration techniques for CBCT-based dose calculation. Strahlenther Onkol 2015;191:970–8.